

quartz/polymer waveguides offers strong advantages in the measurement of CDOM in seawater. The need to carefully match the refractive indices of natural and reference solutions (very challenging in estuarine waters) can be mitigated or eliminated entirely. It is highly desirable to conduct CDOM measurements using waveguides that do not propagate light across optical interfaces. The best means of achieving this objective is the use of waveguides in which the liquid core is in direct physical contact with walls that have a lower index of refraction than water. Additionally, we note that if such an LCW (i.e., $n_T < n_W$) is itself immersed in water, any light propagating within the Teflon wall will efficiently exit the LCW. In this case, even for poorly collimated light, only light traveling solely within the LCW liquid core will reach the detector. We are currently using an LCW of this design for in situ measurements of analytes in seawater (Steimle et al. pers. comm.). As a final note on the practicality of these waveguides. A 50-cm quartz/polymer LCW is currently sold commercially for roughly US \$1300, whereas a 50-cm length of a Teflon AF-2400 LCW costs approximately US \$100.

Robert H. Byrne and Eric Kaltenbacher

College of Marine Science
University of South Florida
140 Seventh Avenue South
St. Petersburg, Florida 33701

Limnol. Oceanogr., 46(3), 2001, 742–745
© 2001, by the American Society of Limnology and Oceanography, Inc.

Liquid capillary waveguide application in absorbance spectroscopy (Reply to the comment by Byrne and Kaltenbacher)

Liquid capillary waveguides (Fig. 1b) have been used in marine applications to determine dissolved characteristics of seawater (D'Sa et al. 1999; Zhang 2000). Byrne and Kaltenbacher (2001) in comparing optical characteristics of type I (Fig. 1a) and type II (Fig. 1b) waveguides attribute spectral nonlinearities in absorbance measurements with type II waveguides to the quartz capillary tubing. We show in this study through a theoretical analysis that in the absence of imperfections in the quartz capillary or the presence of scattering particles in the solution being measured, light cannot be trapped in the waveguide quartz wall as suggested by Byrne and Kaltenbacher. In addition, we present results from laboratory observations that clearly indicate linearity over a wide absorbance and spectral range, including absence of wavelength dependence in the absorption measurements with the quartz/Teflon waveguide. A direct comparison of the two waveguide systems discussed by Byrne and Kaltenbacher was not possible, as no experimental results were shown by them to support their hypothesis.

In D'Sa et al. (1999), we use a quartz capillary tubing ($n_Q = 1.46$ at 589 nm) with an inner diameter of 550 μm , a wall thickness of 50 μm having an outer Teflon AF coating (n_p

References

- D'SA, E. J., R. G. STEWARD, A. VODACEK, N. V. BLOUGH, AND D. PHINNEY. 1999. Determining optical absorption of colored dissolved organic matter in seawater with a liquid capillary waveguide. *Limnol. Oceanogr.* **44**: 1142–1148.
- GREEN, S. A., AND N. V. BLOUGH. 1994. Optical absorption and fluorescence properties of chromophoric dissolved organic matter in natural waters. *Limnol. Oceanogr.* **39**: 1903–1916.
- STONE, J. 1972. Optical transmission in liquid-core quartz fibers. *Appl. Phys. Lett.* **20**: 239–240.
- TSUNODA, K., A. NOMURA, J. YAMADA, AND S. NISHI. 1989. The possibility of signal enhancement in liquid absorption spectrometry with a long capillary cell utilizing successive total reflection at the outer cell surface. *Appl. Spectrosc.* **43**: 49–55.
- WATERBURY, R. D., W. YAO, AND R. H. BYRNE. 1997. Long path-length absorbance spectroscopy: Trace analysis of Fe(II) using a 4.5 m liquid core waveguide. *Anal. Chim. Acta* **357**: 99–102.
- YAO, W., AND R. H. BYRNE. 1999. Determination of chromium (VI) and molybdenum (VI) in natural and bottled waters using long pathlength absorbance spectroscopy (LPAS). *Talanta* **48**: 277–282.
- , ———, AND R. D. WATERBURY. 1998. Determination of nanomolar concentrations of nitrate and nitrite in natural waters using long pathlength absorbance spectroscopy. *Environ. Sci. Technol.* **32**: 2646–2649.

= 1.31 at 589 nm) and an effective path length of 45.9 cm. Fused silica optical fibers having core diameter of 400 μm and a numerical aperture (NA) of 0.22 (589 nm) are used to couple light into and out of the type II waveguide in such a way that no light is coupled into the front face of the high refractive index fused silica quartz capillary wall (Fig. 1b). For seawater, the half-angle α of the source optical fiber emission cone (D'Sa and Lohrenz 1999) is related to its NA in air ($\sin \alpha'$) by the relation

$$n_{sw} \sin(\alpha_{sw}) = \sin(\alpha'). \quad (1)$$

For the real index of refraction of seawater ($n_{sw} = 1.339$), we obtain $\alpha_{sw} = 9.45^\circ$, and thus $\theta_1 = 80.55^\circ$ (for the sum of all light rays coming from the fiber, θ_1 can vary from 80.55° to 90° for a parallel light ray [refer to Byrne and Kaltenbacher, fig. 2]). At the boundary between seawater and the quartz wall, the relation between θ_1 and θ_2 is given by

$$\sin \theta_2 / \sin \theta_1 = n_{sw} / n_Q. \quad (2)$$

Substituting values in Eq. 2, we obtain $\theta_2 = 64.7^\circ$ for $\theta_1 = 80.55^\circ$ and $\theta_2 = 66.5^\circ$ for light emitted along waveguide axis with $\theta_1 = 90^\circ$. Thus, it can be assumed that for an optical

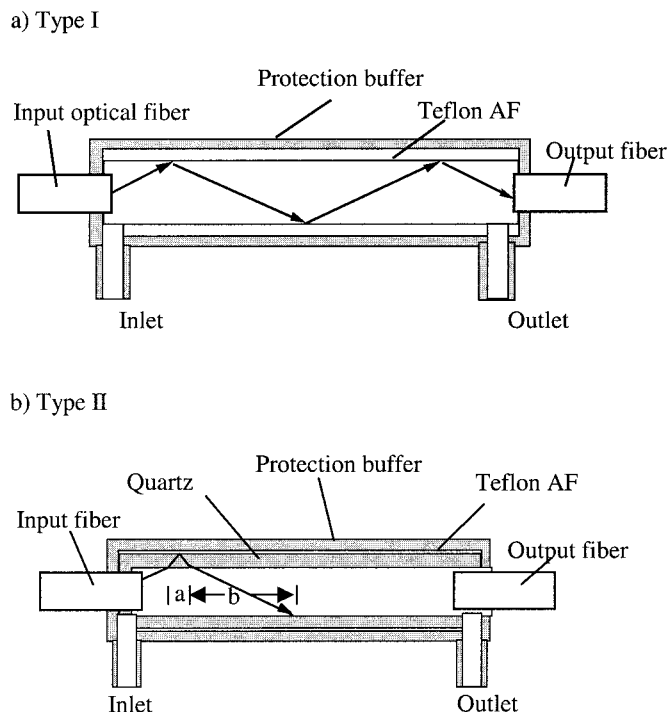


Fig. 1. Cross-sectional view showing light transmission in (a) type I liquid capillary waveguide constructed with solid Teflon AF tubing, and (b) type II capillary waveguide that uses a quartz capillary tubing with an outer coating of Teflon AF. Fluid inlet and outlet and a protective buffer for the two waveguide systems are also shown.

fiber perfectly aligned in the waveguide, $64.7^\circ \leq \theta_2 < 66.5^\circ$ for any light coupled into its quartz wall. For the occurrence of total internal reflection at the quartz/polymer interface, from Snell's law the following inequality should be satisfied, i.e.,

$$\sin \theta_2 > n_p/n_Q, \quad (3)$$

i.e., $\theta_2 > 63.8^\circ$. With $64.7^\circ \leq \theta_2 < 66.5^\circ$ derived from Eq. 2, it can be concluded that there will always be total internal reflection at the quartz/Teflon interface for the conditions of the ideal fiber coupling into the waveguide. This reflected light will then return to the quartz/water interface. For total internal reflection to take place at the quartz/water interface that could result in light being trapped in the waveguide quartz wall,

$$\sin \theta_2 > n_{sw}/n_Q, \quad (4)$$

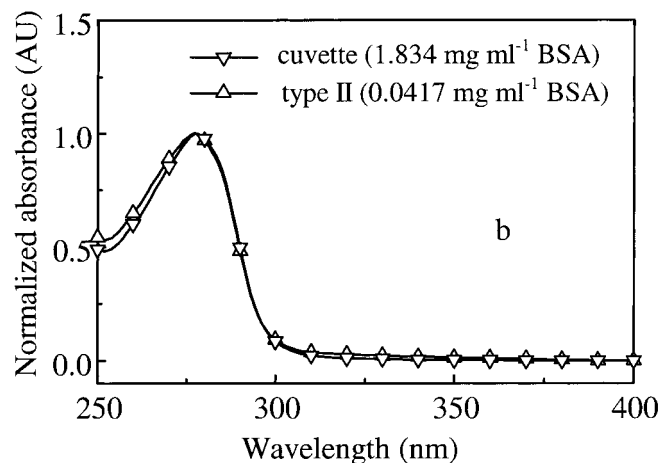
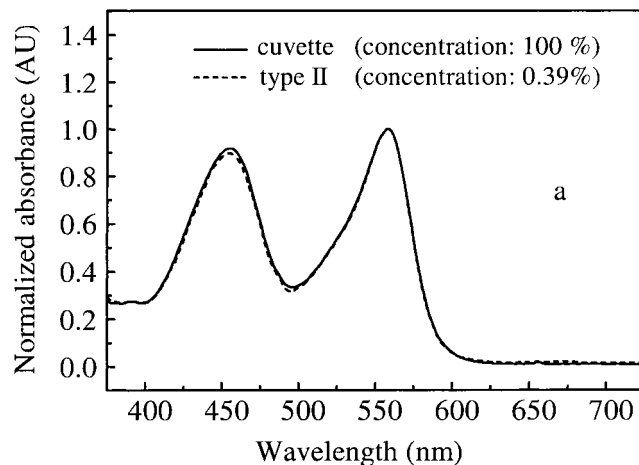


Fig. 2. (a) Normalized absorbance spectra of PhR and HPTS mixture measured with a 1-cm cuvette (100% concentration) and a 50-cm type II capillary waveguide (0.39% relative concentration). (b) Normalized absorbance as a function of wavelength (250–400 nm) for a stock solution of BSA (bovine serum albumin) measured with a 1-cm cuvette (1.834 mg ml⁻¹) and a 50-cm long type II capillary waveguide (0.0417 mg ml⁻¹).

i.e., $\theta_2 > 66.5^\circ$. From Eq. 2, $64.7^\circ \leq \theta_2 < 66.5^\circ$, i.e., θ_2 will always be less than 66.5° , and thus there will never be total internal reflection at the quartz/water interface. Owing to fi-

Table 1. Regression coefficients (*A*, intercept; *B*, slope; *R*², squared correlation coefficient; and *SD*, standard deviation) for the calibration curves of Fig. 3a,b measured with a type II waveguide and a dilution series of PhR/HPTS mixture (*n* = 7) and BSA (*n* = 6).

Wavelength (nm)	Dye	Regression coefficients			
		<i>A</i> (AU)	<i>B</i> (1/AU)	<i>R</i> ²	<i>SD</i> (AU)
400	PhR/HPTS	0.00067	0.104	0.9999	0.0011
456	PhR/HPTS	-0.00167	0.385	0.9999	0.0016
500	PhR/HPTS	-0.00048	0.136	0.9999	0.0010
558	PhR/HPTS	-0.00233	0.431	0.9999	0.0018
280	BSA	-0.05402	28.76	0.9997	0.0109

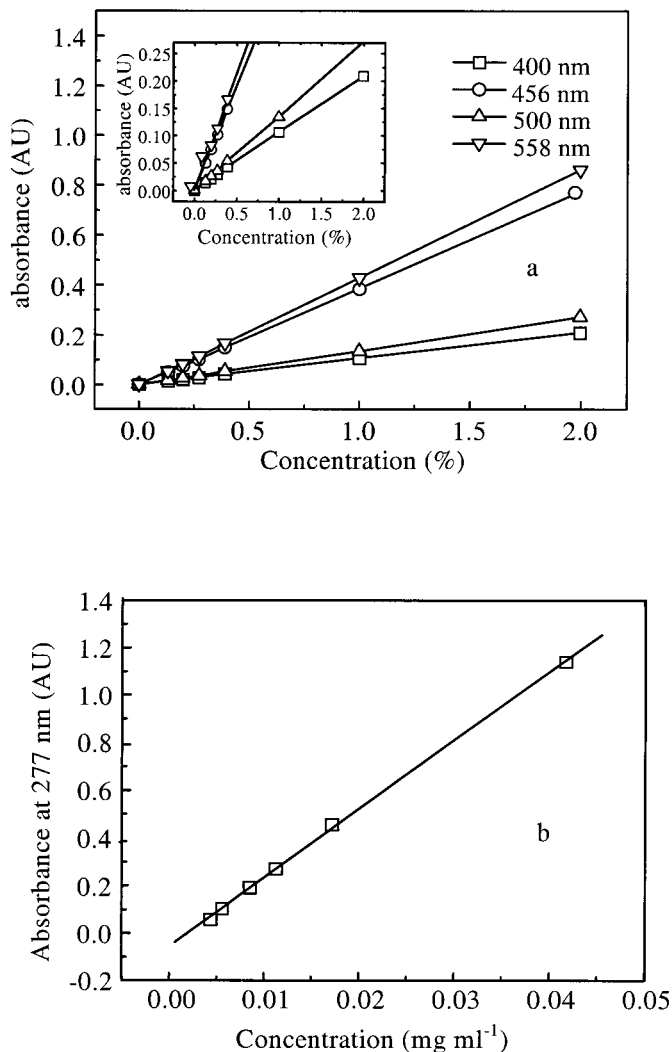


Fig. 3. (a) Calibration curves (*see Table 1* for corresponding regression coefficients) for absorbance as a function of concentration obtained by precision dilution of PhR/HPTS mixture for a 50-cm type II waveguide at four wavelengths (400, 456, 500, and 558 nm). Inset: same linearity at low absorbance range (0.0 to 0.25 absorbance units [AU]). (b) Calibration curve obtained by precision dilution of BSA for the same waveguide.

ber misalignment or the fiber end face being polished accidentally at a slight angle, (possible in type I and type II waveguides) θ_1 can increase slightly. As long as $\theta_2 > 63.8^\circ$, and therefore $\theta_1 > 78.1^\circ$, there will be total internal reflection at the quartz/Teflon interface. If $\theta_1 < 78.1^\circ$, light will penetrate into the Teflon AF layer at θ_3 . However, the Teflon AF layer of type II waveguides used in our experiments (e.g., LCWW-II, World Precision Instruments, Florida) is routinely encapsulated with a buffer coating to secure it against accidental damage during assembly and usage. This buffer coating effectively absorbs light reaching the Teflon AF/buffer coating interface.

The same holds true for measurements with distilled Milli-Q water. Only the distance a and b (Fig. 1b, path lengths in quartz glass and seawater) may vary slightly. However, in

comparison to the different propagating modes from the emitting optical fiber, this variation (i.e., $64.7^\circ \leq \theta_2 < 66.5^\circ$) is negligible. The only concern we have at this point is that the variation in refractive index (freshwater to seawater) will change the NA of the fibers from 0.165 to 0.164 and this will decrease the cones of emission or acceptance of the fibers used for coupling light into and from the waveguide (half-angle α will decrease from 9.52° to 9.45°). This could potentially affect measurements if the fibers are not properly aligned or the numerical aperture of the system is not optically matched (Belz et al. 1999). A possibility exists that this could be one of the reasons for the baseline shift described in D'Sa et al. (1999). This could however also concern measurements with type I waveguides. The only consequence light has traveling in the quartz wall is that the effective path length of the waveguide is slightly shorter than the physical path length. Belz et al. (1999) determined the effective path length of the quartz/Teflon waveguide used in our publication experimentally to be 0.94 of its physical path length, showing that the quartz wall has a minor effect on the waveguide properties.

To fully examine the wavelength dependence of type I and type II waveguides, a ray-tracing model would take into account the complex wavelength-dependent refractive indices of deionized water, seawater, quartz, and Teflon AF, as well as coupling characteristics of the source and detector optical fibers. This exceeds the scope of this reply. We show experimental results that support our theoretical observations. A comparison is made between absorbance spectra obtained with a 1-cm cuvette and a type II waveguide with an effective optical path length of 50 cm. These were connected to a high precision benchtop spectrophotometer (Tidas II, World Precision Instruments) with a built-in cuvette holder and fiber-optic connectors that couple via two 400- μm core diameter optical fibers to the waveguide. Two dyes were selected to generate an absorbance in the 400 to 600 nm range and to allow baseline observation and detection at 700 nm. Stock solution was prepared from phenol red (phenosulfonephthalein) and HPTS (8 hydroxy1,3,6-pyrenetrisulfonic acid trisodium salt), buffered at a pH of 10 to obtain absorbance reading in the 0.8 AU region with a 1-cm cuvette. Further, stock solutions of BSA (bovine serum albumin) were prepared in a phosphate buffer to analyze linearity and effective path lengths in the UV (250 to 300 nm) for the type II waveguide used in our experiments. Spectral absorbance measurements made using a 1-cm cuvette and a 50-cm type II waveguide are normalized and shown in the visible for the PhR/HPTS mixture (Fig. 2a) and in the UV for BSA solution (Fig. 2b). It can be clearly seen that the spectra overlap well. The calibration curves (Fig. 3a) obtained using a dilution series of a mixture of phenol red (PhR) and HPTS shows a strong linearity even at low absorbance values (*see inset of Fig. 3a*). Similar linearity is observed for a dilution series of BSA in the UV (Fig. 3b).

From the standard deviation of the calibration curves it can be concluded that the repeatability of this waveguide is smaller than 2 mAU in the visible and better than 11 mAU in the UV at 280 nm (Table 1). Correlation factors better than 0.9999 obtained in the visible (400 to 600 nm), and

better than 0.99997 in the UV at 280 nm strongly prove that type II waveguides are linear devices within this error range. The effective path length of this waveguide was determined to be 0.95 at 558 nm and 0.94 in at 278 nm respectively, which is within the accuracy obtainable by the dilution method used and agrees well with the results measured by Belz et al. (1999). It can be concluded that type II waveguides are linear within the UV and visible region of the light spectrum used.

Potential advantages of using quartz/Teflon over Teflon only waveguide relate to issues of waveguide contamination and bubble formation (Belz et al. 1999; Zhang 2000). In the case of quartz/Teflon waveguide, cell surface contamination will not alter waveguide properties, whereas the hydrophilic surface of the inner silica surface reduces internal air bubble formation. Teflon AF has a water contact angle of 106° , thus creating a very strong hydrophobic force to trap air bubbles in type I cells. The smaller the air bubble, the stronger it would stick to the internal surface of the waveguide, resulting in baseline shifts. Zhang (2000) used this advantage of type II waveguides for seawater nitrite and nitrate trace analysis by adapting the waveguide to operate as a gas-segmented continuous flow autoanalyzer.

Eurico J. D'Sa and Robert G. Steward

University of South Florida
College of Marine Science
St. Petersburg, Florida 33701

References

- BELZ, M., P. DRESS, A. SUKHITSKIY, AND S. LIU. 1999. Linearity and effective optical pathlength of liquid waveguide capillary cells. *In* Architectures for chemical sensors, Proc. Soc. Photo-Opt. Instrum. Eng. **3856**: 271–281.
- BYRNE, R. H., AND E. KALTENBACHER. 2001. Use of liquid core waveguides for long pathlength absorbance spectroscopy: Principles and practice. *Limnol. Oceanogr.* **46**: 740–742.
- D'SA, E. J., AND S. E. LOHRENZ. 1999. Theoretical treatment of fluorescence detection by a dual-fiber-optic sensor with consideration of sampling variability and package effects associated with particles. *Appl. Opt.* **38**: 2524–2535.
- , R. G. STEWARD, A. VODACEK, N. V. BLOUGH, AND D. PHINNEY. 1999. Determining optical absorption of colored dissolved organic matter in seawater with a liquid capillary waveguide. *Limnol. Oceanogr.* **44**: 1142–1148.
- ZHANG, J.-Z. 2000. Shipboard automated determination of trace concentrations of nitrite and nitrate in oligotrophic water by gas-segmented continuous flow analysis using a liquid waveguide capillary flow cell. *Deep-Sea Res.* **47**: 1157–1171.